



Canadian Journal of Forest Research

Cost implications of cluster plot design choices for precise estimation of forest attributes in landscapes and forests of varying heterogeneity

Journal:	<i>Canadian Journal of Forest Research</i>
Manuscript ID	cjfr-2020-0509.R1
Manuscript Type:	Article
Date Submitted by the Author:	14-Apr-2021
Complete List of Authors:	Lister, Andrew; Northern Research Station, Forest Inventory and Analysis Leites, Laura; Penn State, Ecosystem Science and Management
Keyword:	cluster plot design, forest inventory design optimization, forest inventory cost model, forest pattern simulation, forest sampling simulation
Is the invited manuscript for consideration in a Special Issue? :	Not applicable (regular submission)

SCHOLARONE™
Manuscripts

1 **Cost implications of cluster plot design choices for precise**
2 **estimation of forest attributes in landscapes and forests of varying**
3 **heterogeneity**

4
5 **Andrew J. Lister^{1*} and Laura P. Leites²**

6 *¹ USDA Forest Service, Northern Research Station, Forest Inventory and Analysis,*
7 *3460 Industrial Dr., York, PA 17402, USA*

8 *² Department of Ecosystem Science and Management, Penn State University, 312 Forest*
9 *Resources Bldg., University Park, PA 16802, USA*

10 *Corresponding author: Tel: +1 484 254 6358; Email: andrew.lister@usda.gov

11

Draft

Abstract

12
13
14
15
16
17
18
19
20
21
22
23
24
25
26
27
28
29

Tradeoffs occur when deciding between improving forest inventory precision by increasing sample size or by augmenting cluster plot design factors like size or subplot separation distance. The nature of these tradeoffs changes with variation in type and scale of the spatial pattern of the attribute of interest. In order to understand the impacts of relationships between type and scale of spatial heterogeneity and cluster plot design efficiency, we constructed a factorial simulation experiment and analysed relationships between forest inventory cost, cluster plot design factors, and different spatial heterogeneity scenarios constructed via simulation. To calculate cost, we constructed a cost model that accounted for both on- and between-plot costs. We found that type and scale of heterogeneity have important implications for plot design choices. Homogeneous stands and landscapes are the least-costly to inventory. Subplot area and count have stronger impacts than subplot separation on cost efficiency, particularly in landscapes with aggregated forest patterns and in stands with homogeneous tree patterns. We discuss results in the context of the physical interaction between cluster plot geometry and spatial patterns at different scales, provide computer code for simulations, and suggest principles that forest inventory cluster plot design specialists should consider when designing inventories.

30 **Keywords:** cluster plot design; forest inventory design optimization; forest inventory cost model;
31 forest pattern simulation; forest sampling simulation

32

Introduction

33
34

35 Forest inventories are becoming increasingly important as countries seek to generate
36 information for policy and management decisions, as well as participate in incentives programs
37 aimed at reducing carbon emissions (IPCC 2006; GFOI 2016; FAO 2017). Technical and logistical

38 challenges occur when designing inventories that cover a mosaic of areas with different types and
39 scales of spatial heterogeneity. Clear, science-based guiding principles are therefore needed to
40 develop inventory systems that cost-effectively meet users' needs and function across a broad range
41 of tree and forest spatial pattern conditions.

42 There are several existing frameworks that have been proposed for designing efficient forest
43 inventories. The most common design approach is constructing the inventory to meet precision
44 constraints for the least cost (Freese 1962; Wiant and Yandle 1980; Lynch 2017a). Precision
45 constraints, commonly termed allowable error (AE), are typically presented as the desired
46 confidence interval, sampling error or margin of error of the estimate that will arise from the
47 inventory, along with an associated confidence level. For example, the Intergovernmental Panel on
48 Climate Change recommends an AE of 10% at the 95% confidence level for defensible estimates of
49 carbon stock change (IPCC 2006). AE is used in a straightforward manner in the inventory design
50 process, through the following equation:

$$n_{req} = \left(\frac{CV\% \times t}{AE\%} \right)^2 \quad (1)$$

53
54 where n_{req} is the sample size required to achieve a specified percent standard error (AE%), CV is a
55 known or hypothesized coefficient of variation (CV) of the attribute of interest, and t is the Student's
56 t -value associated with the chosen confidence level (Loetsch and Haller 1973).

57 A key challenge in choosing optimal inventory and plot designs is that relationships between
58 precision of the estimate and plot design change under different attribute spatial heterogeneity
59 scenarios, and it is difficult to predict how these changes will occur (Kleinn 1994; Yim et al. 2015).
60 Sources of heterogeneity include fine scale tree patterns (Stoyan and Penttinen 2000), as well as
61 forest patch patterns at the landscape scale (Riitters et al. 2016). Many forest inventories, like the
62 national forest inventory of the United States, distribute plots across all lands in a spatially-balanced
63 way, including in nonforest areas, since one goal is to monitor forest area dynamics (Bechtold and

64 Patterson 2005). Nonforest values under this paradigm are therefore included as valid plot-level
65 measurements of zero for the attribute of interest (e.g., forest tree density or volume); this
66 contributes, along with variance from measurements within forest patches, to the overall variance
67 of the estimates.

68 The use of cluster plots further complicates forest inventory design decisions. In single stage
69 cluster designs, primary units (sampling units, often referred to as plots) are composed of more than
70 one secondary unit (measurement units, often referred to as subplots) distributed in a consistent
71 pattern such as a line, cross, or L-shape. Cluster plots are generally more efficient because, for the
72 same area measured, they can potentially capture more of the variability that is found on the
73 landscape by avoiding sampling redundant information in spatially-autocorrelated patches (Kangas
74 and Maltamo, 2006; Thompson, 2012). Cluster plot design parameters include subplot size, count,
75 and separation distance. Varying these parameters affects inventory costs, such as those accrued
76 during plot and subplot establishment and walking between subplots.

77 The effect of each of these design parameters on inventory efficiency is hard to predict
78 because of the interaction of different design variables and environmental heterogeneity scale and
79 type. Impacts of cluster plot design on precision have previously been studied using data from
80 mapped stands (Schreuder et al. 1987; Zenner and Peck 2009; Picard et al. 2018), existing forest
81 inventory plots (e.g., Lynch, 2003 ; Picard et al., 2004; Yim et al., 2015), and simulated forest tree
82 patterns (Arvanitis and O'Regan 1967; Mackisack and Wood 1990; Brink and Schreuder 1992; Hou et
83 al. 2015; Gove 2017). Based on our review of the literature, however, there are no studies that use a
84 factorial simulation experiment to model the relationship between plot design parameters, spatial
85 heterogeneity type and scale, and inventory efficiency and costs. Such an experimental approach
86 would allow for control over plot design and heterogeneity scenario parameters, without
87 confounding factors that are common in studies that rely wholly on field measurements. This would
88 increase understanding of the complex relationships among these variables and provide insight into
89 the mechanisms that govern their impacts on inventory efficiency.

90 In this study, we modelled inventory cost as a function of landscape- and stand-scale
91 heterogeneity factors and cluster plot design variables including subplot area, count of subplots, and
92 subplot separation distance. The main goal was to reveal how combinations of these factors and
93 their interactions with scale and type of heterogeneity affect cost, and to provide insights that can
94 help guide the development of efficient inventory networks under different heterogeneity scenarios.

95

96

Methods

97

Simulation Experiment

99

100 A repeated measures factorial simulation experiment with multiple crossed factors (Oehlert
101 2000 p. 438) was conducted in order to model forest inventory cost as a function of two spatial
102 heterogeneity factors and three cluster plot design factors. Each of the two spatial pattern factors,
103 representing landscape (**L**) and stand (**S**) scale heterogeneity, had three levels (Figure 1):

104

105 **L1**: highly dispersed patterns of forest patches with many small, isolated fragments

106 **L2**: intermediate levels of aggregation

107 **L3**: highly aggregated patterns, with large, continuous forest patches

108 **S1**: highly dispersed (uniformly distributed) pattern of tree locations

109 **S2**: completely random pattern of tree locations

110 **S3**: highly aggregated pattern of tree locations, with trees occurring in clumps.

111

112 For each of the 9 factor level combinations, 30 replicates were generated via simulation for a
113 total of 270 replicates (procedure described in the section on simulation details and Figure 1, below).
114 Each of the 270 replicate heterogeneity scenarios was sampled once using systematic sampling with
115 49 plot locations and a cluster plot design arising from every combination of the following factors:

116

117 ***d***: 10, 25 or 50 m subplot separation (measured between subplot edges)118 ***m***: 2, 3, 4 or 5 subplots per plot119 ***a***: 0.01 or 0.2 ha subplot area.

120

121 In other words, each member of a set of $3(\mathbf{d}) \times 4(\mathbf{m}) \times 2(\mathbf{a}) = 24$ cluster plot designs were
122 used to sample each of the 270 replicates at the 49 plot locations, as shown conceptually in Figure 1.
123 This process required a repeated measurements design, as the 49 plot locations were always the
124 same on each replicate; the only thing that changed was the cluster plot design.

125 The variable recorded for each of the $30 \times 3(\mathbf{L}) \times 3(\mathbf{S}) \times 3(\mathbf{d}) \times 4(\mathbf{m}) \times 2(\mathbf{a}) = 6480$ observations
126 was CV of trees per hectare (hereafter, *N*), calculated from the 49 plot-level values and using simple
127 random sampling estimators under a single stage cluster sampling paradigm (Thompson, 2012). CV
128 was chosen because it is needed to estimate the required sample sizes (n_{req} , Eq. 1). Required sample
129 size and plot design parameter costs were used to calculate total inventory cost, the dependent
130 variable we used in our models, for each of the 6480 samples. A summary of this experiment is as
131 follows:

132

- 133 1. Simulate 270 replicates of the forested heterogeneity scenarios (9 ***L-S*** combinations x 30
134 replicates each, Figure 1a).
- 135 2. Overlay a 7 x 7 grid of plot locations on each replicate.
- 136 3. Sample each of the 270 replicates at the plot locations from step 2 using each of the 24
137 cluster plot designs, recording CV of *N* for each case (Figure 1b), leading to 6480
138 observations of CV.
- 139 4. Use Eq. 1 to calculate required sample size (n_{req}) for each observation to achieve an AE of
140 10% sampling error at the 95% level.

- 141 5. Using knowledge of n_{req} , landscape size, and various estimates of on- and between-plot
142 costs, implement a cost model (described in the Cost Model section, below, and Appendix 1)
143 to calculate total inventory cost for each observation.
- 144 6. Build and interpret a linear model of total inventory cost as a function of L , S , d , m , and a .

145

146 <Approximate location of Figure 1>

147

148 *Simulation procedure*

149

150 Simulation of L

151 To create a heterogeneity gradient from simulated landscapes, we used the multifractal map
152 generation feature of the qRule landscape analysis software (Gardner, 2017, 1999). We created
153 square maps (10.24 km sides, 105 km²) with 50% coverage of each of two landcover classes: forest
154 and non-forest. The software generates realistic maps using a fractal algorithm that produces
155 randomized, spatially-correlated patterns of land cover, with the option of controlling the level of
156 aggregation. This allows for the creation of each level of L described above and in Figure 1. We
157 calibrated this algorithm such that the three levels of aggregation corresponded with a gradient of
158 approximate forest edge densities of 432.5 m·ha⁻¹ for **L1**, 55.0 m·ha⁻¹ for **L2**, and 11.2 m·ha⁻¹ for **L3**.
159 Forest edge density is defined as the length of the interface between forest and nonforest pixels,
160 divided by the area of the map. We chose the proportion forest (50%) and edge density parameters
161 to reflect a range of realistic landscape patterns such as those found in Northeastern U.S. temperate
162 forests that intermingle with agricultural and urban areas (e.g. L2 and L3), and those found in
163 silvopastoral ecosystems like those in Central America with sparse tree clusters of different sizes
164 (L1). We provide examples of these types of landscapes and provide code for calculating edge
165 density and forest proportion from existing maps in Supplementary Material S1a.

166 For each level of L , 90 maps (replicates) were simulated, 30 per level of S . The raster
167 (Hijmans, 2019) and spatstat (Baddeley and Turner, 2005) R packages were used to convert the
168 qRule output files to raster objects.

169

170 Simulation of S

171 For the simulations of tree patterns, an N of 388 trees·ha⁻¹ was chosen. This is the average
172 tree density of live trees greater than or equal to 12.7 cm diameter at breast height on forest land
173 for Pennsylvania, according to the USDA Forest Service's Forest Inventory and Analysis (FIA)
174 database (USDA 2020). We considered other commonly reported inventory attributes to use for our
175 study, including basal area per hectare (hereafter, G) and volume per hectare (hereafter, V). N was
176 chosen because, in Pennsylvania, the variance of its estimate for trees greater than 12.7 cm
177 diameter at breast height tends to be slightly higher than that for G but slightly lower than that for V
178 (USDA 2020). In addition, N and G are co-equal components of stocking calculations, making it
179 arguably one of the fundamental forest inventory attributes (Zarnoch and Bechtold 2000).
180 Finally, simulating patterns of N is possible using standard point process models that reflect naturally
181 occurring patterns, while simulating G and V adds complexity by requiring hierarchical models (Lister
182 and Leites 2018) or approaches like the use of copulas (Kershaw et al. 2010) that incorporate effects
183 of tree characteristics in spatial pattern generation.

184 Stoyan and Penttinen (2000) describe how various ecological conditions can lead to regular,
185 random, or dispersed patterns of trees. Regular patterns would occur in plantations with a uniform
186 spacing, or in ecosystems where competition has a repulsive effect on the establishment of
187 individual trees. Random patterns can occur at various seral stages in different ecosystems; Lister
188 and Leites (2018) found that mid-sized trees exhibited random patterns in a secondary growth forest
189 in Pennsylvania, USA. Clustering can occur due to gap dynamics and patterns of mortality and
190 recruitment (Reich and Arvanitis 1992; Larson et al. 2015). To create a heterogeneity gradient from
191 tree spatial patterns at the stand-scale, spatial point process models were used to simulate the three

192 types of **S** pattern types described above at each plot location using the *spatstat* R package. To
193 create the highly dispersed pattern (**S1**), a simple sequential inhibition pattern generator (*rssl*) with a
194 4-m inhibition distance (as might occur in a plantation) and the requisite number of points to
195 achieve the target N was implemented. For the intermediate level of aggregation (**S2**), a
196 homogeneous Poisson process pattern generator (*rpoispp*) was used with the target N to create a
197 completely random spatial pattern (as might occur at various times in forest succession, or with mid-
198 sized trees in some forests (Lister and Leites 2018)). To create the aggregated spatial pattern (**S3**), a
199 Thomas cluster process generator (*rThomas*) was used with a scale parameter of 3 meters, a mean
200 number of points per cluster of 10, and the requisite N for cluster centers. The scale parameter
201 affects the compactness of the clusters; to compare our parameter choice to those that might be
202 found in natural forests, we conducted the analysis described in Supplementary Material S1b.

203 For each level of **S**, 90 realizations (replicates) were generated, 30 per level of **L**. For each of
204 the 49 plots in each of the **L-S** replicates, simulations were performed in a rectangular, 144.7-m x
205 523.6-m window surrounding each cluster plot center. This window size, which represents a 50-m
206 buffer around the largest candidate cluster plot design's footprint, was chosen to minimize artefacts
207 in the point pattern simulation process that would occur from restricting the simulation to the plot
208 boundaries.

209

210 Cluster plot design creation

211 At each plot location, cluster plots with different **d-m-a** configurations at each of 49
212 locations were superimposed over the simulated **L-S** combinations, as shown in Figure 1b, using the
213 *spatstat*, *raster* (Hijmans 2019) and *sp* (Pebesma and Bivand 2005) packages. Cluster plot shapes
214 consisted of a linear array of square subplots aligned north to south (Figure 1). Candidate cluster plot
215 designs were located one at a time, and N for that cluster plot recorded.

216 We have provided R code in Supplementary Material S2 for generating the cluster plot
217 designs and **L-S** scenarios, and for sampling each **L-S-d-m-a** combination. This code can be used to

218 conduct trials with different combinations of the parameters and calibrate cost models that are
219 appropriate to specific situations.

220

221 *Cost model*

222

223 The details of the cost model used are described in Appendix 1. The cost modelling approach
224 used in this study follows that of Zeide (1980) and Wiant and Yandle (1980), which is based
225 principally on the proportions of on- and between-plot times. To make the proposed framework
226 more accessible to practitioners, salary and daily cost rates are included in the cost model. This
227 model is not meant to fully represent reality, but rather to serve as a tool with which to assign a
228 reasonable total inventory cost (the dependent variable used in the linear model) to each of the
229 6480 factor combinations described above, taking into account on-plot, between-plot, and logistical
230 costs. The components of the cost model include:

- 231 1. On-plot costs. These are calculated for each cluster plot design-replicate combination based
232 on assumptions about crew salaries and walking and measurement times required to
233 measure all the trees in a given simulated pattern.
- 234 2. Between-plot costs. These are calculated using the time required to visit all plots for a given
235 cluster plot design-spatial heterogeneity scenario, based on the size of the study area, travel
236 speeds, crew salaries, and n_{req} (Eq. 1).

237 Total inventory cost is calculated as the combination of on- and between-plot costs, as well as daily
238 logistical costs associated with the length of time spent executing the inventory.

239

240 *Analysis*

241

242 Version 3.1-2 of the lmerTest package of version 3.5.1 of the R statistical software (Bates et
243 al. 2015; Kuznetsova et al. 2017; R Core Team 2018) was used to fit the linear model of the form

244

$$245 \quad Cost_{ijkpqr} = \mu + L_i \times S_j \times m_p \times d_q \times a_r + \gamma_{k(ij)} + \delta_{pk(ij)} + \delta_{qk(ij)} + \delta_{rk(ij)} + \varepsilon_{pqrk(ij)} \quad (2)$$

246

247 where Cost is the total inventory cost associated with the kth replicate, for the ith and jth levels of **L**

248 and **S**, respectively, and for the p, q, and rth level of the plot design variables **m**, **d**, and **a**

249 respectively; μ is the overall mean; γ is the replicate random effect with k=1-30 replicates; **L** is the

250 landscape heterogeneity class with i=1-3 levels; **S** is the stand heterogeneity class with j=1-3 levels;

251 **m** is the number of subplots with p=1-4 levels; **d** is the distance between subplots with q=1-3 levels;

252 **a** is the subplot area with r=1-2 levels; $\delta_{p(k)}$, $\delta_{q(k)}$, and $\delta_{r(k)}$ are random effects accounting for

253 repeated measures for **m**, **d** and **a**, respectively; and $\varepsilon_{pqrk(ij)} \sim N(0, \sigma^2)$ is the whole model error term.

254 After the full model was fit, model terms that were not significant were removed, the model was fit

255 again, and modelling assumptions were evaluated using diagnostic graphics.

256

257

Results

258

259 Linear modelling results, which consider the repeated measures factorial design, indicate

260 that landscape- and stand-level heterogeneity scale and type, as well as plot design factors,

261 significantly affect cost, alone and in several interactions (Table 1). Model diagnostic graphics are

262 provided in Supplementary Material S3. In the following sections, we present a summary of the

263 effect of each main factor on cost by averaging across the other factors' levels, highlight the

264 important interactions found, and then characterize the relationship between cost and n_{req} .

265

266

<Approximate Location of Table 1>

267

268 *Impacts of L and S on costs and n_{req}*

269

270 Landscape-scale heterogeneity **L** has a significant effect on inventory cost (Table 1). The
271 more aggregated landscape patterns (**L2** and **L3**) both require a higher (by 102 and 122%,
272 respectively) average cost and higher (by 74 and 85%, respectively) average n_{req} to achieve AE than
273 does the dispersed landscape type (**L1**, Figure 2). The level of variability of the cost values
274 (interquartile range (IQR) and range) suggests that plot design decisions have an important effect on
275 cost in all **L-S** combinations, particularly in **L2** and **L3**, where the ranges of cost are over 100% larger
276 than that of the more dispersed **L1** (Figure 2). However, ranges and IQRs of n_{req} are similar across **L**
277 levels, suggesting that design choices have less potential impact on n_{req} in different landscape types.

278 Stand-scale tree pattern **S** also has a significant impact on inventory cost (Table 1). As with
279 landscape pattern, average cost and n_{req} increase with increasing level of stand pattern aggregation
280 (**S1-S3**). Average cost generally increases linearly; however, there is a much larger (20%) increase in
281 mean n_{req} between **S2** and **S3** compared to that between **S1** and **S2** (4%). Within each **L** level, ranges
282 and IQRs of cost are similar across levels of **S**, but those of n_{req} are much larger for **S3** (Figure 2). This
283 suggests that cluster plot design decisions have similar potential impact on inventory cost in
284 different stand pattern types, but have very different potential impacts on n_{req} , particularly for the
285 aggregated stand type. This is the opposite of what results suggest for landscape pattern
286 aggregation, where cost variability is more sensitive than that of n_{req} to landscape pattern
287 differences.

288

289 <Approximate location of Figure 2>

290

291 *Impacts of plot design factors on costs and n_{req}*

292

293 Of the three plot design variables evaluated, subplot area a was the most impactful, with the
 294 mean cost of 0.01 ha subplots being 71% lower than that of 0.2 ha subplots (Figure 3). Compared to
 295 smaller subplots, ranges and IQRs of cost were much larger for 0.2 ha subplots, indicating that
 296 varying the other plot design factors can have high impacts when designing inventories with large
 297 subplots.

298 For the smaller subplots size (0.01 ha), increasing stand aggregation (from **S1** to **S3**), lead to
 299 a high cost range and IQR. This increase in cost range and IQR in more aggregated stand patterns is
 300 of less magnitude when subplot size was larger (0.2 ha). This trend is reversed as landscape
 301 aggregation increases (from **L1** to **L3**); cost variability was relatively stable for small subplots but
 302 increased dramatically between **L1** and **L3** for large subplots (Figure 3). These findings are reinforced
 303 by the highly significant interaction between a and S and between a and L (Table 1), and highlight
 304 the complex relationships between design factors and attribute spatial patterns.

305 Subplot area a and number of subplots m interact significantly (Table 1), which was
 306 expected as they determine total plot area. The highest mean cost plot design was the one with the
 307 largest total plot area ($a=0.2, m=5$) while the lowest mean cost was for the nearly smallest total plot
 308 area ($a=0.01, m=3$) (Figure 4). The situation is reversed for n_{req} : the design with highest n_{req} was for
 309 the smallest plot ($a=0.01, m=2$), while the lowest n_{req} was for the largest plot ($a=0.2, m=5$) (Figure 5).
 310 To summarize, results indicate that as a general pattern, increasing number of subplots and subplot
 311 area (and thus total plot area) increases cost and decreases n_{req} (Figures 4 and 5).

312

313 <Approximate Location of Figure 3>

314 <Approximate Location of Figure 4>

315 <Approximate Location of Figure 5>

316

317 The effect of number of subplots on cost and n_{req} are also mediated by the heterogeneity
 318 type and level (Figures 4 and 5); this is supported by the significant $a:m:L$ and $a:m:S$ interactions

319 from the model results (Table 1). As landscape aggregation increases from **L1** to **L3**, the cost impact
320 of raising the number of subplots increases, dramatically so for larger subplot sizes (Figure 4). The
321 same pattern of cost increase is observed as stand aggregation level increases, however, to a lesser
322 extent. This suggests that cluster plot design decisions about number and size of subplots should
323 thus be made by focusing more on the coarser-scale landscape pattern structure than on fine-scale
324 stand patterns.

325 The above-described patterns of cost are reversed for n_{req} ; increasing the number of
326 subplots has a larger impact on n_{req} as stand-scale aggregation increases from **S1** to **S3**, dramatically
327 so for smaller subplot sizes (Figure 5). The same pattern of higher impact of m is observed as
328 landscape aggregation level increases, however, to a lesser extent. The opposing results when
329 evaluating cost vs. n_{req} highlight the importance of including both cost analyses and precision in
330 design decisions.

331 Subplot separation (d) is the least impactful of the design variables studied. Although d
332 occurs in several significant interactions in our model (Table 1), the practical effect of varying d is
333 relatively small (Figures 4 and 5). In general, as distance between subplots increases, the cost and
334 the n_{req} decrease. However, the magnitude of this effect generally depends on the size of the
335 subplots: for large subplots, increasing d has a larger impact on cost (Figure 4) and a smaller impact
336 on n_{req} (Figure 5).

337

338

Discussion

339

340 This study uncovers the nature of the effects of spatial heterogeneity on inventory plot
341 design efficiency, highlighting that decisions related to plot design should be considered in the light
342 of landscape and stand level heterogeneity. Depending on the type and level of heterogeneity, the
343 decisions regarding subplot size, number and separating distance have different importance.

344 Other studies have used either mapped or simulated stands to assess the effects of spatial
345 pattern at the plot-scale (Henttonen and Kangas 2015; Häbel et al. 2019). Our study is unique
346 because we deliberately construct a broad range of spatial patterns at two scales, using tools offered
347 by point process (Baddeley et al. 2015) and landscape pattern modelling (Gardner 1999), that reflect
348 very different forest heterogeneity scenarios (Figure 1). As in large scale inventories that seek to
349 monitor conversions to and from forest, like that of the USDA Forest Service's FIA program (USDA,
350 2020), plots in our study often fell partially or entirely within nonforest gaps, contributing
351 significantly to the variance of estimates, calling into question design guidelines constructed with
352 results from studies in homogeneous areas.

353

354 *Impacts of landscape heterogeneity **L** and stand heterogeneity **S** on costs*

355

356 Figure 2 shows that there are important differences between mean costs across **L** levels, and
357 smaller differences in mean cost across **S** levels. Both landscape- and stand-level pattern aggregation
358 raise inventory costs. Less-aggregated landscapes (**L1**) are on average the least costly to inventory,
359 and these costs are relatively insensitive to plot design choices. This is shown by how a broad range
360 of n_{req} leads to a much narrower range of cost relative to the more aggregated landscape pattern
361 types. For intermediate **L2** and aggregated **L3** landscapes, this situation is different; there are
362 generally broad ranges of cost differences relative to the range of required sample sizes, indicating
363 that design choices affecting CV and thus n_{req} are more important in landscapes with aggregated
364 forest patterns.

365 Uniform stands (**S1**) are on average the least costly to inventory, followed by stands with
366 random tree patterns (**S2**); both are less costly than inventories in stands with clustered patterns
367 (**S3**) (Figure 2). Uniform and random tree patterns have similar cost- n_{req} relationships, as we
368 expected, because as analysis windows get larger, point density estimates from random patterns
369 tends to converge with those obtained from uniform patterns much faster than do those from

370 aggregated patterns (Wiegand and Moloney 2014). At the scale of plots (i.e., analysis windows) and
371 with the average tree densities used in this experiment, means from the random pattern resemble
372 those of the uniform pattern. Had we used lower tree densities, or smaller plots, differences would
373 have been greater.

374 Our results align with those of other studies. In a study using a sampling simulation on a set
375 of stem-mapped tropical forest stands, Picard et al. (2018) found that spatial pattern variations due
376 to differing forest types and stand structures had strong impacts on the CV-plot size relationships
377 and cost optimality of different designs, with coarse-scale heterogeneity effects being stronger than
378 those of local-scale heterogeneity. Similarly, Baraloto et al. (2013) found meaningful differences in
379 plot design-variance relationships across five neotropical forests, and much smaller differences
380 within each forest. Häbel et al. (2019) found that costs are lowest in more regular stands than in
381 clustered or random stands, and that increasing subplot size had a larger impact on precision in
382 clustered patterns than in homogeneous patterns. Clearly, these findings depend upon the nature of
383 the heterogeneity introduced at each scale; sharp forest/nonforest boundaries will have a greater
384 variance-inducing effect than will finer-scale variations in levels of forest attributes that do not
385 create gaps into which entire plots or subplots fall.

386

387 *Impacts of interactions between design factors, L , and S on costs*

388

389 Effects of m and a

390 The overall pattern of change in cost and n_{req} with plot area is largely due to the well-known
391 inverse exponential relationship between plot area and CV (and thus n_{req}) identified by Smith (1938)
392 and several others; as plots get larger, there is a diminishing rate of reduction in variance. However,
393 increasing plot size incurs costs, and the results indicate that, depending upon L - S type, the CV and
394 n_{req} reduction benefits of increasing plot size do not balance out the additional field costs incurred
395 when plots get very large. This finding motivates a recommendation to use clusters that are

396 significantly smaller than 1 ha, which are commonly recommended, when cost function parameters
397 and attribute variance structure resemble those from our experiment.

398 Several authors have found that cost optimization favoured smaller plots ranging in size
399 from 0.07 to 0.2 ha (Mesavage and Grosenbaugh 1956; Scott 1993; Yim et al. 2015; Lynch 2017b).
400 Others have found that in areas with extreme levels of between-plot costs, or to meet needs like
401 measuring site-based diversity or calculating stand indices that require more trees to be meaningful,
402 plots between 0.25 and 2 ha might be required (Zenner and Peck 2009; Rejou-Mechain et al. 2014;
403 Picard et al. 2018). In addition, if inventory plots are to be linked to remote sensing data and used to
404 train models, larger plots help mitigate the effects of spatial mismatch between plots and pixels
405 (Næsset et al. 2015; GFOI 2016).

406 Given this broad range of recommendations, it becomes clear that studies like this one, that
407 not only assess different designs in a methodical way, but also experimentally integrate different
408 heterogeneity scenarios, can help reveal mechanisms behind cost efficiency. For example, the
409 results of our study indicate that as landscape aggregation level and thus forest patch sizes increase,
410 cost-plot size relationships vary in alignment with principles identified in the conceptual model
411 shown in Figure 6a. In the more-aggregated **L3** landscape type, increasing subplot size is less likely to
412 cause the plot to represent a microcosm of the larger study area than it is in **L1**, so while costs on the
413 plot increase, n_{req} and cost between plots does not decrease as much as it does in **L1** (Figure 4,
414 Figure 5, Figure 6a). If each plot's status is more similar to that of the landscape as a whole, as in **L1**,
415 its contribution to variance and CV will be smaller, leading to, on average, fewer and/or less costly
416 plots needed to achieve AE requirements from the sample.

417 For stand-scale aggregation **S**, similar principles apply. At higher stand aggregation levels
418 (**S3**), Figure 4 reveals an important phenomenon: a negative exponential pattern of the relationship
419 between cost and number of subplots in the panel associated with smaller subplots, and a positive
420 relationship in the panel associated with larger subplots. This suggests that the optimal (lowest cost)
421 plot size lies somewhere between 0.05 ha (five 0.01 ha subplots) and 0.4 ha (two 0.2 ha subplots).

422 This supports the hypothesis that increasing plot size in aggregated stands makes each plot more like
423 a microcosm of the stand-scale patterns found on the landscape than it does in the stands where
424 trees are more evenly-distributed like **S1** and **S2** (Figure 6b), where the optimum plot size generally
425 appears to be at or below 0.01 ha. For both **L** and **S**, there is therefore little cost advantage to
426 increasing plot size unless the heterogeneity type is such that reductions in CV and subsequent
427 savings in n_{req} offset the on-plot cost increases from measuring larger plots.

428

429 <Approximate location of Figure 6>

430

431 Effects of d

432 Separating subplots has a similar effect on variance as does increasing plot area, but for
433 slightly different reasons. In theory, separating subplots should lead to the mean landscape
434 condition being captured more efficiently for the same total plot area because the cost inefficiencies
435 associated with measuring redundant information in spatially-autocorrelated patches should be
436 mitigated (Cochran 1977; Kleinn 1994; Tokola 1999; Yim et al. 2015). In practice, the magnitude of
437 the impacts of subplot separation distance on CV and cost is linked to the relationship between it
438 and the spatial structure of the resource under study and the relative costs associated with walking
439 between subplots.

440 Increasing landscape aggregation (from **L1** to **L3**) leads to a reduction of cost benefits from
441 subplot separation (Figure 4). As with increasing plot size, separating subplots is more likely to
442 capture the variability found on the landscape, reducing variance, when forest patches are more
443 dispersed, like in **L1**. However, separating subplots found in large, aggregated forest or nonforest
444 patches (**L2** and **L3**) will lead to less reduction of variance and in n_{req} , but higher on-plot costs from
445 additional walking. This will tip the balance and favour lower values of d in more aggregated
446 landscapes (Figure 6c). As levels of stand-scale heterogeneity increase (**S1** to **S3**), subplot separation

447 becomes more cost-advantageous, because in more aggregated stands, subplots move into or out of
448 patches of trees over relatively short distances (Figure 6d).

449

450 *Additional considerations*

451

452 We used approaches similar to others who have built cost models for forest inventories
453 (Zeide 1980; Scott 1993; Zhang et al. 1994; Yim et al. 2015; Yang et al. 2017), and attempted to
454 provide estimates of cost parameters that were reasonable based on personal experience and
455 discussions with field inventory personnel. However, there are several factors for which we did not
456 account. First and foremost, our cost model is based on the use of fixed area cluster plot designs
457 with the cost parameters we selected. These model parameters would vary if different field
458 techniques (lasers for distance/height measurements vs. tapes and clinometers, or variable radius
459 vs. fixed area plots) were used. Yang et al. (2017) and Lynch (2017b) report that for the datasets
460 they examined, there was a rather flat optimality region associated with the cost (or relative
461 standard error):plot size curve, suggesting that excessive fine tuning of cost and design parameters
462 might not be important in practice. However, Chen et al. (2019) found a much narrower range of
463 optimality, suggesting that under certain heterogeneity scenarios and when costs are a limiting
464 factor, design decisions become more important. Due to the varied influences of inventory methods
465 and attribute heterogeneity on costs, we designed our modelling framework and simulation
466 experiment with enough flexibility to allow for a wide variety of spatial heterogeneity scenarios and
467 user-specified cost model parameters.

468 Another factor that could alter the results of our study is the choice of the attribute on
469 which to optimize. Yang et al. (2017) employ a variable radius plot procedure that focuses sampling
470 effort on tree counts because, particularly for smaller diameter classes, this attribute is generally
471 more variable than volume or basal area. We chose N because, for trees above 12.7 cm in diameter,
472 its variance is intermediate to that of G or V (USDA 2020) and because point pattern simulation of N

473 is much less complex than alternative approaches that include effects of tree size on spatial
474 patterns. In real-world inventories, there are multiple objectives and types of information needs,
475 and it is important to note that different attribute choices will have different variance structures,
476 affecting outcomes of plot design choices.

477 Finally, the logistics of conducting the inventory are crucial determinants of cost efficiency.
478 In the US Forest Service's national forest inventory, for example, plots are pre-screened with aerial
479 imagery before a field crew is sent. In the context of our experiment, this would dramatically reduce
480 the impact of n_{req} , as many plots that fall entirely within nonforest patches would not require a field
481 visit. The travel logistics are also key; for example, with respect to plot size, higher between-plot
482 travel costs would tend to shift the optimum toward larger plots, as on-plot costs would represent a
483 lower proportion of overall inventory cost (Zeide 1980).

484 Our research provides practical guidance to decision makers. First, the results strongly
485 suggest that a simulation study aimed at modelling the effects of spatial pattern type and scale, plot
486 design factors, and AE requirements on inventory cost can be extremely valuable, as our results
487 show that there are important total inventory cost differences across the range of plot design
488 choices that are often considered. Traditional paradigms of inventory plot design tend to rely on
489 large inventory plots, with the idea that these somehow "capture" rare events or give more accurate
490 estimates of the status of the attribute. What is not considered, however, is that a common goal of
491 an efficient inventory design is not to maximize the unknowable quantity "accuracy", but rather to
492 meet AE requirements for minimum cost. We have therefore provided a conceptual framework, as
493 well as code for conducting simulations, with which practitioners can approach inventory plot design
494 choices in ways that are better than simply resorting to the "bigger is better" orthodoxy.

495 Secondly, we have demonstrated the value of using the tools of point process modelling and
496 landscape simulation for inventory plot design investigations. The importance of the effects of plot
497 design on inventory costs changes with spatial heterogeneity scenario, and while our specific
498 heterogeneity scenarios are not perfect facsimiles of nature, the principles that our simulation

499 experiment reveal and our methods and software code can be used to guide plot design
500 experiments in the field or in future simulation studies. For example, to simulate tree point patterns
501 that resemble those found in a particular study area, a practitioner can either assume that the
502 dominant pattern type can be described by one of the three stand-scale pattern scenarios used in
503 this study (Figure 1), or implement a more sophisticated point process modelling approach using
504 data from stem-mapped plots or stands (Lister and Leites 2018). For example, Henttonen and Kangas
505 (2015) and Häbel et al. (2019) found that plot design optimality varied greatly by combination of
506 inventory attribute and tree size distribution-induced spatial pattern properties.

507 With respect to landscape patterns, our recommendation for practitioners would be to test
508 plot designs using existing forest/nonforest maps in place of simulated maps, because these exist at
509 the appropriate resolution for most areas. For example, by integrating realistic, simulated point
510 pattern maps with realistic land cover maps created from actual landscapes, a reasonable facsimile
511 of the population could be produced and various plot types overlaid and tested using the analysis
512 framework we have presented.

513

514 *Conclusions*

515

516 The type and scale of heterogeneity found in the population being inventoried matters when
517 making plot design choices. In our experiment, landscape-scale heterogeneity affects the magnitude
518 of costs more than stand-scale heterogeneity, with costs increasing with aggregation level. At the
519 stand scale, areas with clustered tree patterns are more costly to survey than those with regular tree
520 patterns, with random tree patterns being intermediate to the two. It is more advantageous to
521 increase plot size in stands with aggregated tree patterns compared to stands with more uniform
522 tree patterns, mainly because there is a larger reduction in CV as plot size, and to a lesser extent
523 subplot separation distance, go up. These relationships are sensitive to the scale of heterogeneity of
524 the attribute of interest, relative to the dimensions of the plot. Subplot count and area are more

525 important design decisions affecting total cost than subplot separation distance, although once plot
526 area has been chosen, separation distance matters, with smaller distances being more cost-effective
527 for smaller plots, and larger distances being more cost-effective for larger plots. This relationship is
528 affected more by landscape than by stand heterogeneity; there is less cost penalty from subplot
529 separation in more uniform landscapes.

530 This study is unique in that it recognizes inventory situations where the paradigm includes a
531 survey of the entire land base including nonforest areas. We designed a simulation experiment
532 framework that allows testing different plot design factor combinations using modelling and
533 simulation tools from the disparate fields of point process modelling and landscape ecology. This
534 study not only reveals how various plot design factors interact under different heterogeneity
535 scenarios to affect costs, but it also provides a conceptual framework and computer code with which
536 to examine these interactions. Our goal was to provide guidance to practitioners and tools that can
537 serve as a foundation for future studies in this important area.

538 **Acknowledgements**

539
540
541 We would like to thank Ephraim Hanks, Eric Zenner, Doug Miller, Charles Scott, James Westfall,
542 Samidha Shetty, Tyler Garner, John Stanovick and two anonymous reviewers for advice and guidance
543 on earlier versions of this manuscript. This work was partially supported by the USDA National
544 Institute of Food and Agriculture and Hatch Appropriations under Project #PEN04700 and Accession
545 #1019151.

546 **References**

547
548
549 Arvanitis, L., and O'Regan, W. 1967. Computer simulation and economic efficiency in forest
550 sampling. *Hilgardia* **38**(2): 133–164. doi:10.3733/hilg.v38n02p133.

- 551 Baddeley, A., Rubak, E., and Turner, R. 2015. Spatial point patterns - Methodology and applications
552 with R. Chapman & Hall/CRC Interdisciplinary Statistics, New York. 828 pp.
- 553 Baraloto, C., Molto, Q., Rabaud, S., Herault, B., Valencia, R., Blanc, L., Fine, P., and Thompson, J.
554 2013. Rapid simultaneous estimation of aboveground biomass and tree diversity across
555 neotropical forests: a comparison of field inventory methods. *Biotropica* **45**(3): 288–298.
556 doi:10.1111/btp.12006.
- 557 Bates, D., Mächler, M., Bolker, B., and Walker, S. 2015. Fitting linear mixed-effects models using
558 lme4. *J. Stat. Softw.* **67**(1): 1–48. doi:10.18637/jss.v067.i01.
- 559 Bechtold, W.A., and Patterson, P.L. eds. 2005. The enhanced forest inventory and analysis
560 program—national sampling design and estimation procedures, GTR-SRS-80. Gen. Tech. Rep.,
561 U.S. Department of Agriculture, Forest Service, Southern Research Station, Asheville, NC. 85 pp.
562 Available from <https://www.fs.usda.gov/treearch/pubs/20371> [accessed 27 November
563 2020].
- 564 Brink, G.E., and Schreuder, H.T. 1992. ONEPHASE: a simulation program to compare 1-phase
565 sampling strategies. Research Paper, USDA Forest Service, Rocky Mountain Forest and Range
566 Experiment Station, Fort Collins, Colorado. Available from
567 <http://catalog.hathitrust.org/Record/011397236>.
- 568 Chen, Y., Yang, T.-R., Hsu, Y.-H., Kershaw, J.A., and Prest, D. 2019. Application of big BAF sampling for
569 estimating carbon on small woodlots. *For. Ecosyst.* **6**(1): 13. doi:10.1186/s40663-019-0172-4.
- 570 Cochran, W. 1977. Sampling techniques. John Wiley & Sons, New York. 428 pp.
- 571 FAO. 2017. Voluntary guidelines on national forest monitoring. Food and Agriculture Organization of
572 the United Nations (FAO), Rome. Available from <http://www.fao.org/3/a-l6767e.pdf>.
- 573 Freese, F. 1962. Elementary forest sampling. USDA Forest Service, Washington, D.C. Available from
574 <https://books.google.com/books?id=wIkWAAAAYAAJ>.

- 575 Gardner, R.H. 1999. RULE: Map generation and a spatial analysis program. *In* Landscape ecological
576 analysis: Issues and applications. *Edited by* J.M. Klopatek and R.H. Gardner. Springer, New York,
577 NY. pp. 280–303. doi:10.1007/978-1-4612-0529-6_13.
- 578 GFOI. 2016. Integration of remote-sensing and ground-based observations for estimation of
579 emissions and removals of greenhouse gases in forests: Methods and guidance from the Global
580 Forest Observations Initiative. Food and Agriculture Organization, Rome. Available from
581 <https://www.fs.usda.gov/treesearch/pubs/56461> [accessed 27 November 2020].
- 582 Gove, J. 2017. Some refinements on the comparison of areal sampling methods via simulation.
583 *Forests* **8**(10): 393. doi:10.3390/f8100393.
- 584 Häbel, H., Kuronen, M., Henttonen, H.M., Kangas, A., and Myllymäki, M. 2019. The effect of spatial
585 structure of forests on the precision and costs of plot-level forest resource estimation. *For.*
586 *Ecosyst.* **6**(1): 8. doi:10.1186/s40663-019-0167-1.
- 587 Hasler, M., and Hornik, K. 2007. TSP - Infrastructure for the traveling salesperson problem. *J. Stat.*
588 *Softw.* **23**(2): 1–21.
- 589 Henttonen, H., and Kangas, A. 2015. Optimal plot design in a multipurpose forest inventory. *For.*
590 *Ecosyst.* **2**. doi:10.1186/s40663-015-0055-2.
- 591 Hijmans, R.J. 2019. raster: Geographic data analysis and modeling, version 2.9-23. [https://CRAN.R-](https://CRAN.R-project.org/package=raster)
592 [project.org/package=raster](https://CRAN.R-project.org/package=raster). Available from <https://CRAN.R-project.org/package=raster>
593 [accessed 27 November 2020].
- 594 Hou, Z., Xu, Q., Hartikainen, S., Antilla, P., Packalen, T., Maltamo, M., and Tokola, T. 2015. Impact of
595 plot size and spatial pattern of forest attributes on sampling efficacy. *For. Sci.* **61**(5): 847–860.
596 doi:10.5849/forsci.14-197.
- 597 IPCC. 2006. IPCC guidelines for national greenhouse gas inventories. Institute for Global
598 Environmental Strategies, Japan. Available from [http://www.ipcc-](http://www.ipcc-nggip.iges.or.jp/public/2006gl/)
599 [nggip.iges.or.jp/public/2006gl/](http://www.ipcc-nggip.iges.or.jp/public/2006gl/) [accessed 27 November 2020].

- 600 Kershaw, J.A., Richards, E.W., McCarter, J.B., and Oborn, S. 2010. Spatially correlated forest stand
601 structures: A simulation approach using copulas. *Comput. Electron. Agr.* **74**(1): 120–128.
602 doi:10.1016/j.compag.2010.07.005.
- 603 Kleinn, C. 1994. Comparison of the performance of line sampling to other forms of cluster sampling.
604 *For. Ecol. Manag.* **68**(2–3): 365–373. doi:10.1016/0378-1127(94)90057-4.
- 605 Kuznetsova, A., Brockhoff, P.B., and Christensen, R.H.B. 2017. lmerTest package: tests in linear mixed
606 effects models. *J. Stat. Softw.* **82**(13): 1–26. doi:10.18637/jss.v082.i13.
- 607 Larson, A., Lutz, J., Donato, D., Freund, J., Swanson, M., HilleRisLambers, J., Sprugel, D., and Franklin,
608 J. 2015. Spatial aspects of tree mortality strongly differ between young and old-growth forests.
609 *Ecol.* **96**(11): 2855–2861. doi:10.1890/15-0628.1.
- 610 Lister, A.J., and Leites, L.P. 2018. Modeling and simulation of tree spatial patterns in an oak-hickory
611 forest with a modular, hierarchical spatial point process framework. *Ecol. Model.* **378**: 37–45.
612 doi:10.1016/j.ecolmodel.2018.03.012.
- 613 Loetsch, F., and Haller, K.E. 1973. *Forest inventory*. BLV, Munich, Germany. 469 pp.
- 614 Lynch, A.M. 2003. Comparison of fixed-area plot designs for estimating stand characteristics and
615 western spruce budworm damage in southwestern U.S.A. forests. *Can. J. For. Res.* **33**(7): 1245–
616 1255. doi:10.1139/x03-044.
- 617 Lynch, T.B. 2017a. Optimal plot size or point sample factor for a fixed total cost using the Fairfield
618 Smith relation of plot size to variance. *For. Int. J. For. Res.* **90**(2): 211–218.
619 doi:10.1093/forestry/cpw038.
- 620 Lynch, T.B. 2017b. Optimal sample size and plot size or point sampling factor based on cost-plus-loss
621 using the Fairfield Smith relationship for plot size. *Forestry* **90**(5): 697–709.
622 doi:10.1093/forestry/cpx024.
- 623 Mackisack, M.S., and Wood, G.B. 1990. Simulating the forest and the point-sampling process as an
624 aid in designing forest inventories. *For. Ecol. Manag.* **38**(1): 79–103. doi:10.1016/0378-
625 1127(90)90087-R.

- 626 Mesavage, C., and Grosenbaugh, L.R. 1956. Efficiency of several cruising designs on small tracts in
627 north Arkansas. *J. For.* **54**(9): 569–576. doi:<https://doi.org/10.1093/jof/54.9.569>.
- 628 Næsset, E., Bollandsås, O.M., Gobakken, T., Solberg, S., and McRoberts, R.E. 2015. The effects of
629 field plot size on model-assisted estimation of aboveground biomass change using
630 multitemporal interferometric SAR and airborne laser scanning data. *Remote Sens. Environ.*
631 **168**: 252–264. doi:10.1016/j.rse.2015.07.002.
- 632 Oehlert, G.W. 2000. *A first course in design and analysis of experiments*. W. H. Freeman, New York.
633 679 pp.
- 634 Pebesma, E.J., and Bivand, R.S. 2005. Classes and methods for spatial data in R. *R News* **5**(2): 9–13.
- 635 Picard, N., Nouvellet, Y., and Sylla, M.L. 2004. Relationship between plot size and the variance of the
636 density estimator in West African savannas. *Can. J. For. Res.* **34**(10): 2018–2026.
637 doi:10.1139/X04-079.
- 638 Picard, N., Gamarra, J.G.P., Birigazzi, L., and Branthomme, A. 2018. Plot-level variability in biomass
639 for tropical forest inventory designs. *For. Ecol. Manag.* **430**: 10–20.
640 doi:10.1016/j.foreco.2018.07.052.
- 641 R Core Team. 2018. *R: A Language and Environment for Statistical Computing*, version 3.5.1. R
642 Foundation for Statistical Computing, Vienna, Austria. Available from [https://www.R-](https://www.R-project.org/)
643 [project.org/](https://www.R-project.org/) [accessed 27 November 2020].
- 644 Reich, R.M., and Arvanitis, L.G. 1992. Sampling unit, spatial distribution of trees, and precision.
645 *North. J. Appl. For.* **9**(1): 3–6. doi:10.1093/njaf/9.1.3.
- 646 Rejou-Mechain, M., Muller-Landau, H., Detto, M., Thomas, S., Le Toan, T., Saatchi, S., Barreto-Silva,
647 J., Bourg, N., Bunyavejchewin, S., Butt, N., Brockelman, W., Cao, M., Cardenas, D., Chiang, J.,
648 Chuyong, G., Clay, K., Condit, R., Dattaraja, H., Davies, S., Duque, A., Esufali, S., Ewango, C.,
649 Fernando, R., Fletcher, C., Gunatilleke, I., Hao, Z., Harms, K., Hart, T., Herault, B., Howe, R.,
650 Hubbell, S., Johnson, D., Kenfack, D., Larson, A., Lin, L., Lin, Y., Lutz, J., Makana, J., Malhi, Y.,
651 Marthews, T., McEwan, R., McMahan, S., McShea, W., Muscarella, R., Nathalang, A., Noor, N.,

- 652 Nytch, C., Oliveira, A., Phillips, R., Pongpattananurak, N., Punchi-Manage, R., Salim, R.,
653 Schurman, J., Sukumar, R., Suresh, H., Suwanvecho, U., Thomas, D., Thompson, J., Uriarte, M.,
654 Valencia, R., Vicentini, A., Wolf, A., Yap, S., Yuan, Z., Zartman, C., Zimmerman, J., and Chave, J.
655 2014. Local spatial structure of forest biomass and its consequences for remote sensing of
656 carbon stocks. *Biogeosciences* **11**(23): 6827–6840. doi:10.5194/bg-11-6827-2014.
- 657 Riitters, K., Wickham, J., Costanza, J., and Vogt, P. 2016. A global evaluation of forest interior area
658 dynamics using tree cover data from 2000 to 2012. *Landsc. Ecol.* **31**(1): 137–148.
659 doi:10.1007/s10980-015-0270-9.
- 660 Rosenkrantz, D.J., Stearns, R.E., and Lewis, P.M. 2009. An analysis of several heuristics for
661 the traveling salesman problem. *In* *Fundamental problems in computing: Essays in honor of*
662 *Professor Daniel J. Rosenkrantz. Edited by S.S. Ravi and S.K. Shukla. Springer Netherlands,*
663 *Dordrecht. pp. 45–69. doi:10.1007/978-1-4020-9688-4_3.*
- 664 Schreuder, H.T., Banyard, S.G., and Brink, G.E. 1987. Comparison of three sampling methods in
665 estimating stand parameters for a tropical forest. *For. Ecol. Manag.* **21**(1): 119–127.
666 doi:10.1016/0378-1127(87)90076-4.
- 667 Scott, C.T. 1993. Optimal design of a plot cluster for monitoring. *In* *Proceedings of the IUFRO S.4.11*
668 *Conference. Edited by K. Rennolls and G. Gertner. University of Greenwich, London, UK. pp.*
669 *233–242. Available from <http://www.nrs.fs.fed.us/pubs/42932> [accessed 27 November 2020].*
- 670 Smith, H. 1938. An empirical law describing heterogeneity in the yields of agricultural crops. *J. Agric.*
671 *Sci.* **28**: 1–23. doi:10.1017/S0021859600050516.
- 672 Stoyan, D., and Penttinen, A. 2000. Recent applications of point process methods in forestry
673 statistics. *Stat. Sci.* **15**(1): 61–78. doi:10.1214/ss/1009212674.
- 674 Tokola, T. 1999. Comparison of cluster-sampling techniques for forest inventory in southern Nepal.
675 *For. Ecol. Manag.* **116**(1–3): 219–231. doi:https://doi.org/10.1016/S0378-1127(98)00457-5.
- 676 USDA. 2020. Evalidator retrieval for volume per acre of forest, basal area per acre of forest, and
677 trees per acre of forest for trees greater than 5 inches dbh, Pennsylvania EVALID 422018. Forest

- 678 Inventory and Analysis, U.S. Department of Agriculture, Forest Service, Northern Research
679 Station. Available from <http://apps.fs.usda.gov/Evalidator/evalidator.jsp> [accessed 27
680 November 2020].
- 681 Wiant, H.V., and Yandle, D.O. 1980. Optimum plot size for cruising sawtimber in eastern forests. *J.*
682 *For.* **78**(10): 642–643. doi:10.1093/jof/78.10.642.
- 683 Wiegand, T., and Moloney, K.A. 2014. Handbook of spatial point-pattern analysis in ecology. CRC
684 Press, Taylor & Francis Group, Boca Raton, FL. 512 pp.
- 685 Yang, T.-R., Hsu, Y.-H., Kershaw, J.A., McGarrigle, E., and Dan Kilham. 2017. Big BAF sampling in
686 mixed species forest structures of northeastern North America: Influence of count and measure
687 BAF under cost constraints. *Forestry: An International Journal of Forest Research* **90**(5): 649–
688 660. doi:10.1093/forestry/cpx020.
- 689 Yim, J.-S., Shin, M.-Y., Son, Y., and Kleinn, C. 2015. Cluster plot optimization for a large area forest
690 resource inventory in Korea. *For. Sci. Technol.* **11**(3): 139–146.
691 doi:10.1080/21580103.2014.968222.
- 692 Zeide, B. 1980. Plot size optimization. *For. Sci.* **26**(2): 251–257. doi:10.1093/forestscience/26.2.251.
- 693 Zenner, E.K., and Peck, J.E. 2009. Characterizing structural conditions in mature managed red pine:
694 spatial dependency of metrics and adequacy of plot size. *For. Ecol. Manag.* **257**(1): 311–320.
695 doi:https://doi.org/10.1016/j.foreco.2008.09.006.
- 696 Zhang, R., Warrick, A.W., and Myers, D.E. 1994. Heterogeneity, plot shape effect and optimal plot
697 size. *Geoderma* **62**(1–3): 183–197. doi:10.1016/0016-7061(94)90035-3.

698

699

Appendices

700

701 **Appendix 1.** Cost model and explanation of cost components used to calculate total inventory cost
702 from specific plot design-required sample size scenarios.

703

Table 1. Parameters, *F* statistic and *p*-values associated with the final model from Eq. 2.

Parameter	F-value	p-value	Parameter	F-value	p-value
(Intercept)	24584.4	<.0001	S	272.3	<.0001
a	267293.7	<.0001	L:d	79.48	<.0001
a:L	18747.34	<.0001	m:S	60.04	<.0001
a:m	13262.61	<.0001	a:d	30.27	<.0001
m	3541.28	<.0001	a:m:S	26.61	<.0001
a:m:L	1063.06	<.0001	d	7.17	0.0008
L	873.66	<.0001	a:m:d	6.2	<.0001
m:L	683.1	<.0001	m:d	2.43	0.0239
a:S	497.44	<.0001			

Draft

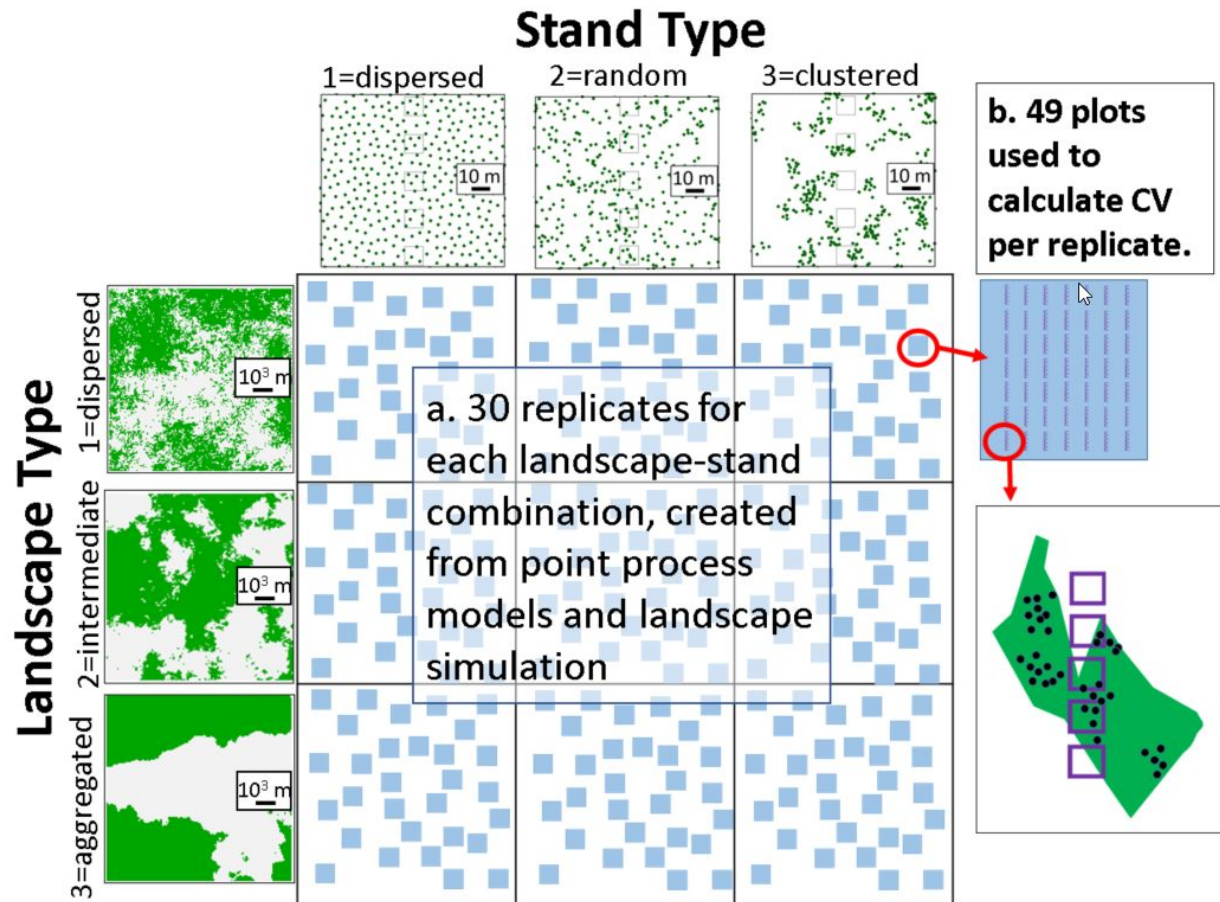


Figure 1. Conceptual model depicting factorial experimental design. a) Thirty replicates for each of 3 levels of landscape-scale (*L*) heterogeneity were simulated for each of 3 levels of stand-scale (*S*) heterogeneity. b) At each plot located on a 7x7 grid superimposed on each landscape, stand-scale patterns were simulated for each level of *S*. Candidate cluster plot designs were superimposed over each plot location for each replicate, and TPH was calculated per plot. CVs from the 49 plots were calculated for each combination of candidate plot design and replicate.

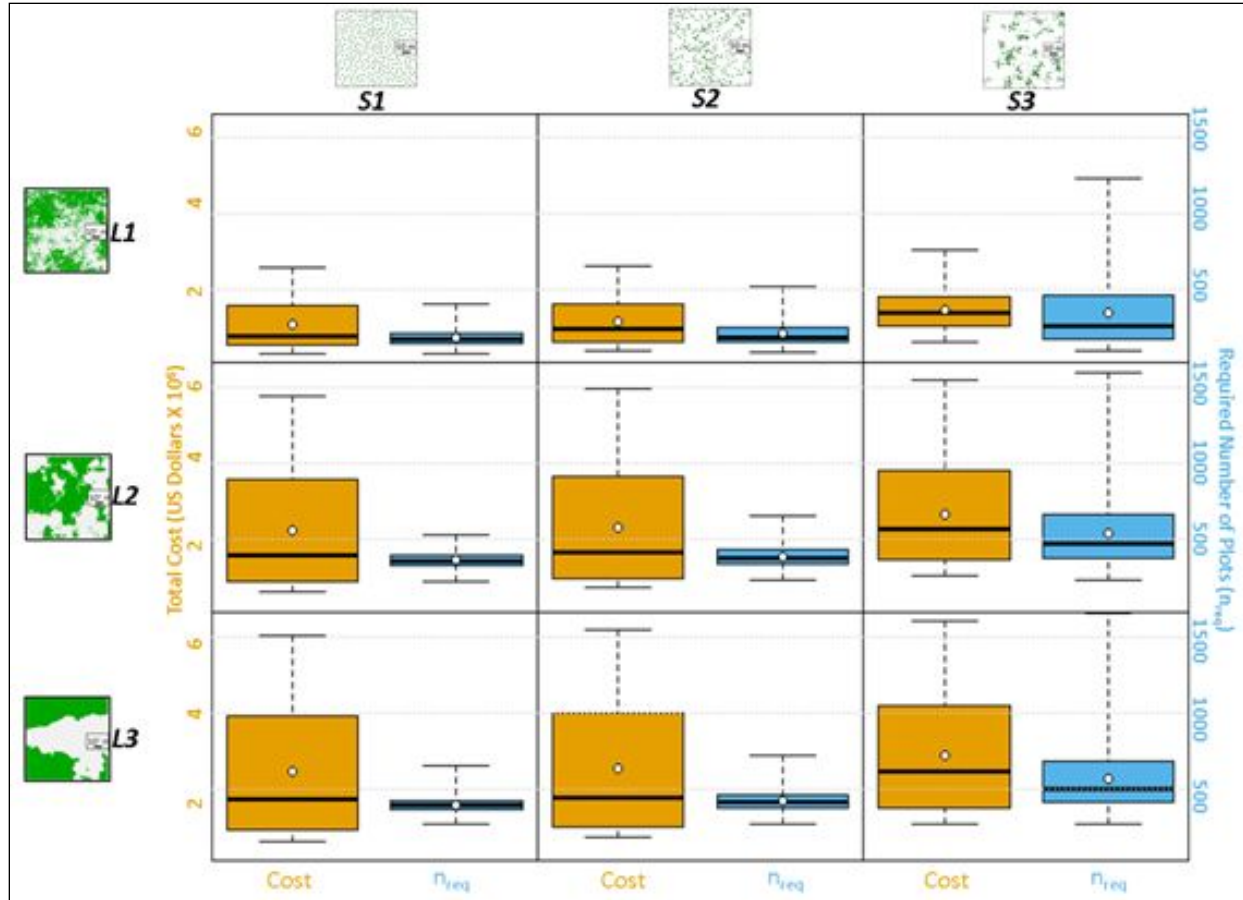


Figure 2. Boxplot of the total inventory cost (orange shading) and required number of plots (n_{req} , blue shading) values for each landscape) and stand heterogeneity type combination. Shaded boxes = interquartile ranges, dark lines = medians, small circles = means, and dashed lines = range of values for each level. $n=2160$ for each level.

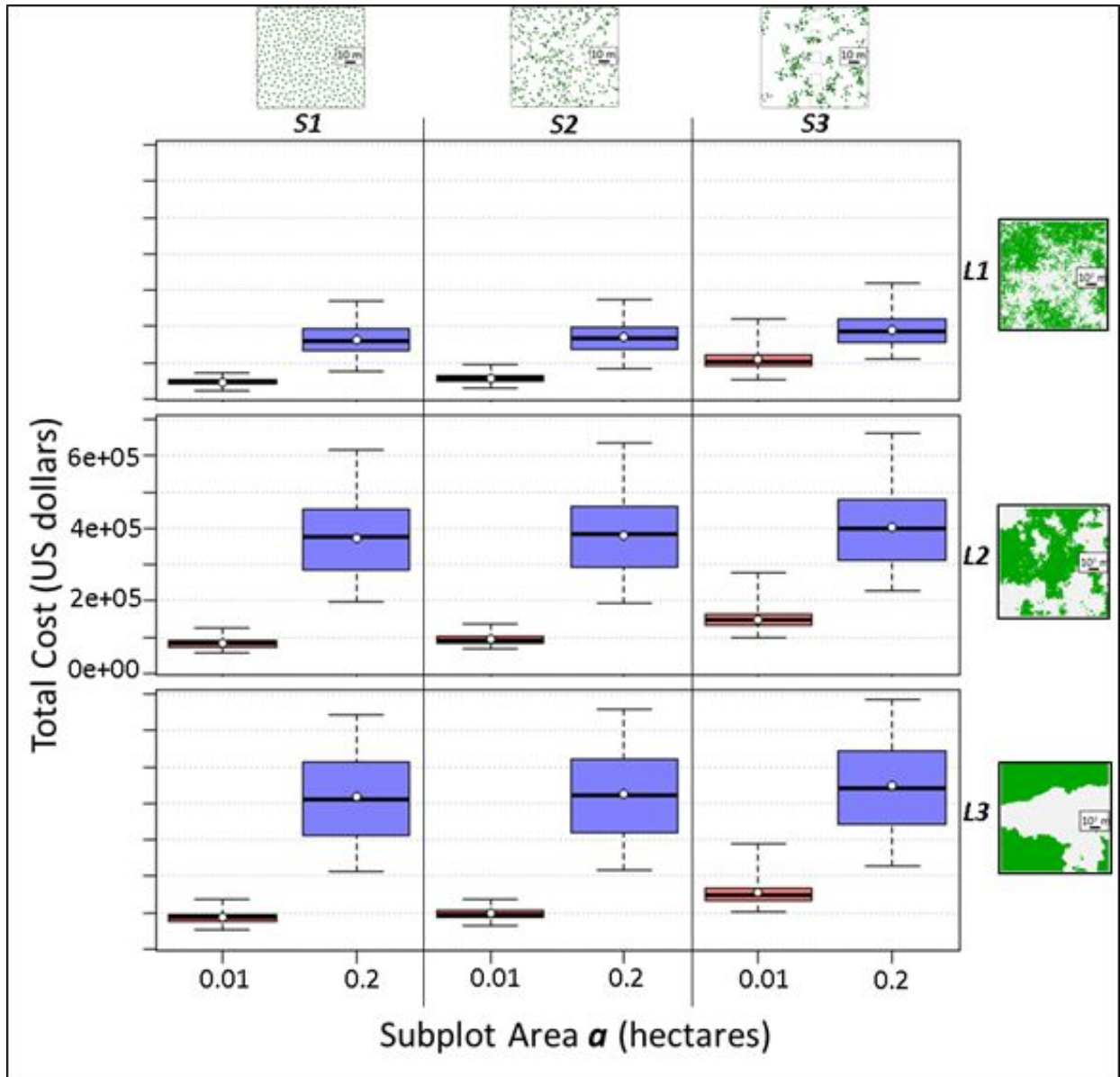


Figure 3. Boxplot representing distribution of total inventory cost values for each combination of subplot area (α), landscape type (*L1*, *L2*, *L3*), and stand type (*S1*, *S2*, *S3*). Shaded boxes = interquartile ranges, dark lines = medians, small circles = means, and dashed lines = range of values for each level.

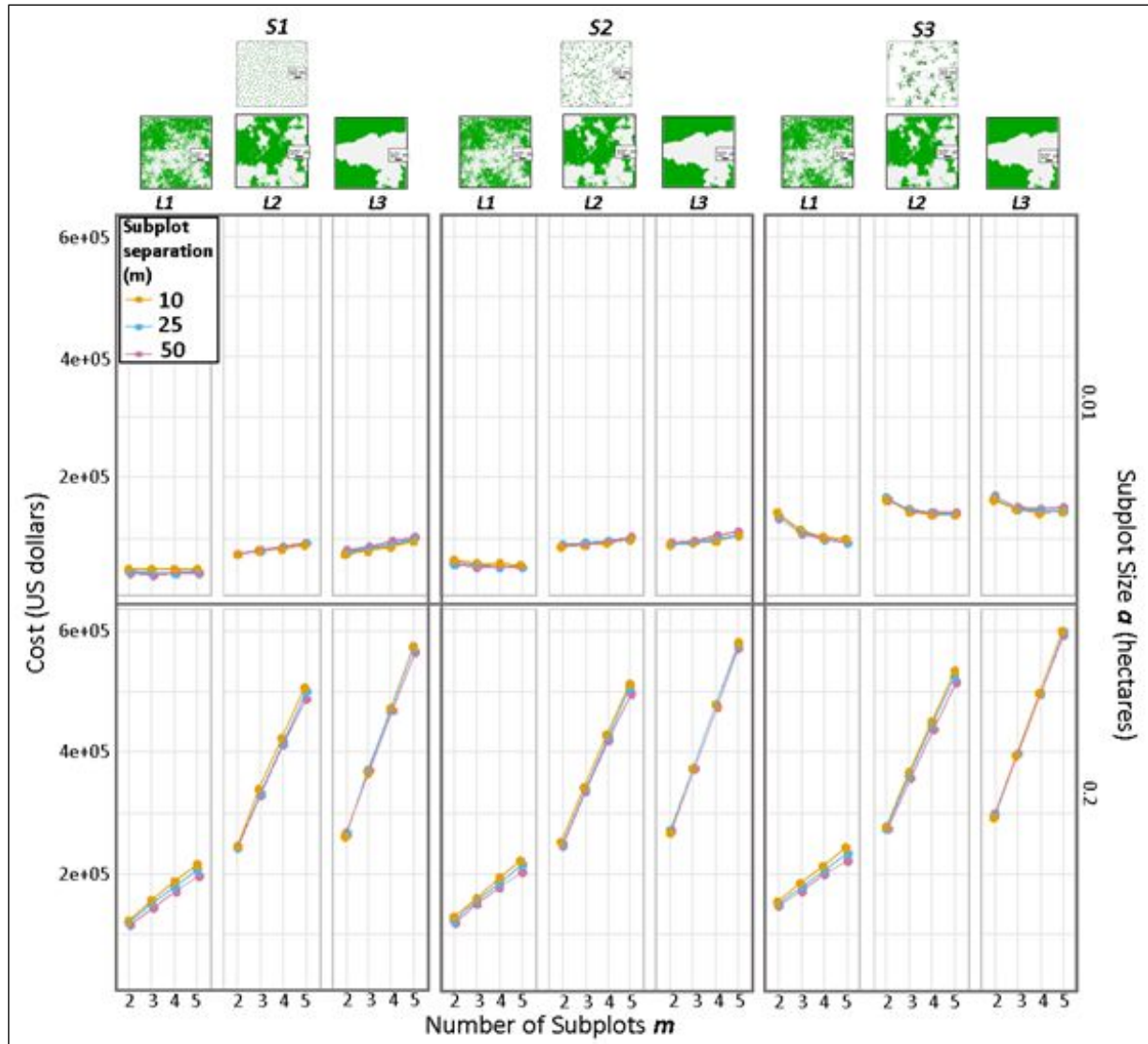


Figure 4. Interaction plots showing the relationship between mean total inventory cost and different levels of the factors used in the simulation (α =subplot area, d =subplot edge separation distance, m =number of subplots, L = landscape type, S = stand type).

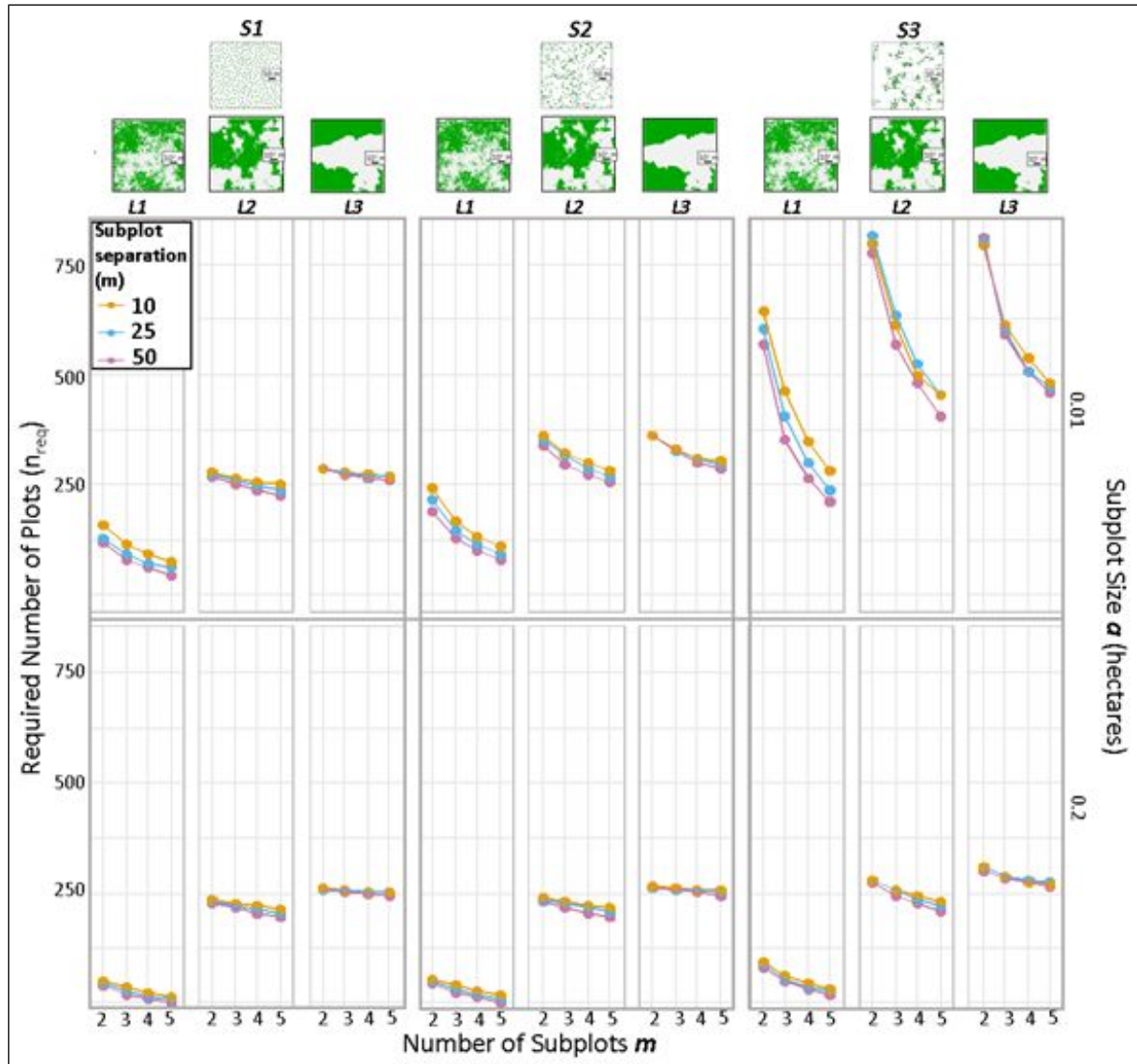


Figure 5. Interaction plots showing the relationship between mean required number of plots (n_{req}) to meet allowable error (AE) and different levels of the factors used in the simulation (α =subplot area, d =subplot edge separation distance, m =number of subplots, L = landscape type, S = stand type).

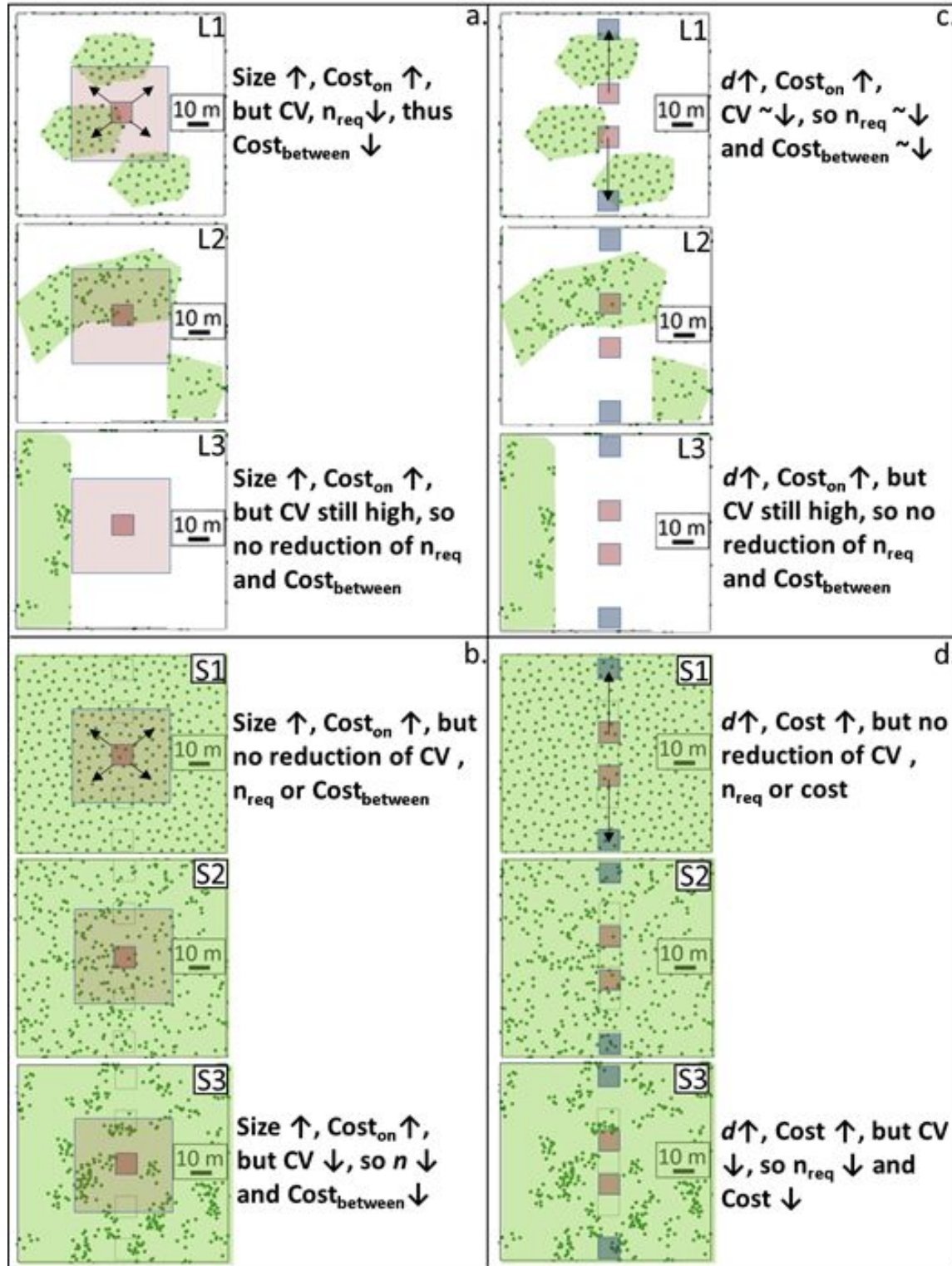


Figure 6. Conceptual model showing hypothesized mechanisms for how increasing plot size and separation affect CV and costs across levels of landscape type (*L*) (a&c) and stand type (*S*) (b&d). Arrows represent increasing of plot size or separation distance from smaller (subplot area (*a*)=0.01 ha) or closer (subplot separation distance (*d*)=10 m) to larger (*a*=0.2 ha) or more separated (*d*=50 m) cluster plot designs. Green areas represent forested areas, small dots represent tree locations.

APPENDIX 1

Cost Model

The cost model used to calculate total inventory cost based on assumptions about crew salaries, work rates, travel rates, and daily logistical costs is described below. The combination of simulated forest pattern and cluster plot configuration leads to on-plot costs, and required sample sizes, along with assumptions about travel speed rates, affect between-plot costs. Daily rates are affected by time required to complete the entire inventory. Assumptions of the cost model are as follows:

1. Plots are visited in succession, with field crews receiving salary for 8 hours per day. At the end of each day, the field crew will lodge at a negligible distance from the route between plots.
2. Logistical costs such as training, equipment purchases, lodging costs, vehicle purchase or lease, and overhead costs, can be subsumed into a daily cost, with the assumption that they can be amortized using the time period that the inventory field data are being collected.
3. Any other costs associated with on- or between-plot work can be subsumed into these components.
4. There is no upper time or cost limit to complete the inventory, as the goal is to seek the design that achieves AE for a single attribute of interest for the minimum cost.
5. A single crew is used to visit all plots; i.e., there are no crews working in parallel.
6. Several additional cost components are not considered in order to avoid excessive complexity, such as additional time required to measure edge trees (Zeide 1980), rest or data entry times, and so on.

The cost model with three terms, reflecting on-plot costs, between-plot costs, and logistical costs, is as follows:

$$C_T = S_c \times n \times T_p + S_c \times [n \times T_t + (n-1) \times T_d] + C_L \times D \quad (A1)$$

where:

C_T = total cost (US dollars)

S_c = total field crew salary (US dollars/hr); this was set to 100\$/hr

n = required number of plots to meet precision requirements, calculated from the CV and Eq. 1

T_p = time (hrs) required on-plot to complete plot (Eq. A3)

T_d = time (hrs) required driving from one plot to the next (Eq. A6)

T_t = transition time spent between leaving vehicle and arriving at plot, then, when finished with measurements, leaving the plot and entering vehicle (round trip time was set to 0.33 hours per plot). Note that separating this factor, which could in principle be combined with driving time into a "between-plot cost" component, allows for experimental manipulation of the on:between plot cost ratio without having to adjust driving velocity.

Logistical cost components:

C_L = logistical costs (US dollars/day); this was set to 200\$/day

D = number of days to complete inventory (Eq. A2)

$$D = [n \times (T_p + T_t) + (n-1) \times T_d] / 8 \text{ hours/day} \quad (A2)$$

Note that logistical components, as we have incorporated them, are in effect daily costs that go up as more days are required to complete the inventory, given the number of required plots and time expenditure required for transportation and field work.

On-plot time components:

$$T_p = (d_t + m \times d_c + d_m) / V_w + T_m \times p \quad (\text{A3})$$

where:

d_t = distance walked along shortest path between trees on the plot, returning to first tree (m) (Figure A1 (a)). This shortest path distance was calculated using an algorithmic solution to what is known as the Traveling Salesperson Problem (TSP), farthest insertion method (Rosenkrantz et al. 2009) found within the R package *TSP* (Hasler and Hornik 2007). This approach was used to find a common method for tracing an efficient route between all of the trees found on a plot, regardless of the spatial pattern, and regardless of the fact that, in practice, field crews will seldom visit trees in this manner. d_t is thus considered to be a reasonable proxy for inter-tree walking time given that spatial patterns of trees differ greatly by level of *S*.

m = number of subplots

d_c = distance from center of subplot to each of 4 corners and back to center (Eq. A4); this is meant to be a simplistic representation of costs associated with marking the corners of a square subplot.

$$d_c = 2 \times [4 \times (0.5 \times \text{sqrt}(2 \times l_s^2))] \quad (\text{A4})$$

where:

l_s = length of one side of a subplot (Figure A1 (b))

d_m = distance between subplot centers and back to sp1 (Eq. A5)

$$d_m = 2 \times [(2 \times (0.5 \times l_s) + d) \times (m-1)] \quad (\text{A5})$$

where:

d = separation distance between subplot sides (Figure A1 (c))

V_w = walking velocity (m/hr); this was set to 1609.5 m/hr

T_m = time spent measuring a tree (hours/tree); this was set to 0.05 hours/tree; we ignore the fact that edge trees will require more time to discern and measure, or that many NFIs will require more measurement time per tree, particularly in dense stands if heights are measured

p = # of trees on a plot

Between-plot driving time components:

$$T_d = [\text{sqrt}(A)/\text{sqrt}(n)]/V_d \quad (\text{A6})$$

where:

A = area (km²) of the population; this was set to 10,000 km² for logistical reasons related to the computational requirements of the simulation, and to provide a large enough area over which to distribute a spatially-balanced sample of 49 points that are assumed to be independent of one another.

V_d = velocity (km/hr) of inter-plot travel; this was set to 48 km/hr.

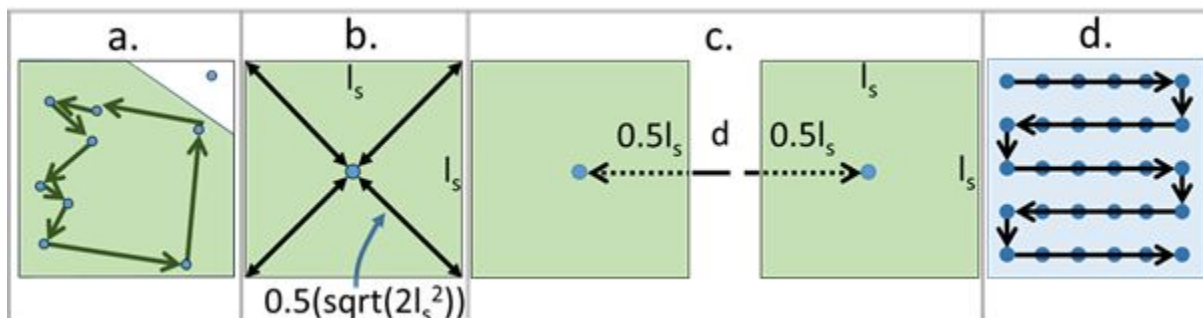


Figure A1. Graphical depiction of components of the cost model used in the study. a. Example of the Travelling Salesman Problem (TSP)-derived shortest distance between a set of forest trees (points)

- 94 found in a forest (green, shaded areas in all graphics; nonforest trees are not measured) (d_t). b.
95 Example of the calculation of subplot establishment walking distance (d_e). c. Example of the walking
96 distance back and forth between two subplot centers (d_m). d. A depiction of the assumed travel
97 route and length of the set of segments that need to be traversed to visit all plots.

Draft